UC Irvine
UC Irvine Previously Published Works

Title
Search for a nearly degenerate lepton doublet (L-,L0)

Permalink
https://escholarship.org/uc/item/8bt586bb

Journal
Physical Review D, 42(1)

ISSN
2470-0010

Authors
Riles, K
Perl, ML
Barklow, T
et al.

Publication Date
1990-07-01

DOI
10.1103/physrevd.42.1

Copyright Information
This work is made available under the terms of a Creative Commons Attribution License, availalbe at https://creativecommons.org/licenses/by/4.0/

Peer reviewed

eScholarship.org Powered by the California Digital Library
University of California

PHYSICAL REVIEW D

PARTICLES AND FIELDS

THIRD SERIES, VOLUME 42, NUMBER 1 1 JULY 1990

Search for a nearly degenerate lepton doublet (L^-, L^0)

K. Riles,[a] M. L. Perl, T. Barklow, A. Boyarski, P. R. Burchat,[b] D. L. Burke, J. M. Dorfan, G. J. Feldman, L. Gladney,[c] G. Hanson,[d] K. Hayes, R. J. Hollebeek,[c] W. R. Innes, J. A. Jaros, D. Karlen,[e] S. R. Klein,[f] A. J. Lankford, R. R. Larsen, B. W. LeClaire,[g] N. S. Lockyer,[c] V. Lüth, R. A. Ong,[h] B. Richter, and J. M. Yelton[i]

Stanford Linear Accelerator Center, Stanford University, Stanford, California 94309

G. Abrams, D. Amidei,[h] A. R. Baden,[j] J. Boyer, F. Butler,[k] G. Gidal, M. S. Gold, G. Goldhaber, L. Golding,[l] J. Haggerty,[m] D. Herrup,[j] I. Juricic,[n] J. A. Kadyk, M. E. Levi, M. E. Nelson,[o] P. C. Rowson,[n] H. Schellman,[j] W. B. Schmidke, P. D. Sheldon,[p] G. H. Trilling, and D. R. Wood[q]

Lawrence Berkeley Laboratory and Department of Physics, University of California, Berkeley, California 94720

T. Schaad[r]

Department of Physics, Harvard University, Cambridge, Massachusetts 02138

(Received 14 August 1989)

We have searched for a heavy charged lepton with an associated neutrino of nearly the same mass in e^+e^- annihilation data taken with the Mark II detector at a center-of-mass energy of 29 GeV. In order to suppress contamination from conventional two-photon reactions, this analysis uses a novel, radiative-tagging technique. Requiring the presence of an isolated, energetic photon allows a search for lepton doublets with mass splittings smaller than that previously accessible to experiment. No evidence for such a new lepton doublet has been found, enabling limits to be placed on allowed mass combinations. Mass splittings as low as 250–400 MeV/c^2 are excluded for charged-lepton masses between 500 MeV/c^2 and 10 GeV/c^2.

I. INTRODUCTION

We reported earlier[1] the results of a search in e^+e^- annihilation data at $\sqrt{s}=29$ GeV from the Mark II detector[2] for a new lepton doublet (L^-, L^0), in the case where the L^0 may be massive but is lighter than the L^-.[3] No evidence for a new lepton doublet was found, but for the case of near degeneracy, when the mass difference

$$\delta \equiv m_- - m_0 \tag{1}$$

is much less than m_-, the earlier search lacked sensitivity because of large backgrounds from two-photon processes. Using a novel radiative-tagging technique in a new search, we have achieved greater sensitivity to the case of near degeneracy.

We assume that the lepton doublet is subject to conventional weak interactions, such that the L^- decays to a L^0 through the emission of a virtual W^- boson, which itself decays to conventional leptons or hadrons. We also assume that the L^0 is unlikely to decay within the Mark II detector, implying a lifetime $\tau(L^0) > 100$ ns. As discussed in Ref. 1, such a lepton doublet is not ruled out by cosmological constraints from the energy density of the Universe. Raby and West[4] have suggested such a doublet with $m_0 \approx 4-10$ GeV/c^2 could explain both the dark-matter and solar-neutrino problems.

Our previous search considered various event topologies, providing sensitivity to both leptonic and hadronic decay modes of the heavy charged lepton. In order to reduce two-photon backgrounds at low visible energies, however, at least one decay in each event was required to produce an isolated electron or muon. Unfortunately, in the case of near degeneracy, the average visible energies of detected particles are low because of the energy lost to the undetected heavy neutrinos. This makes electron and muon identification with the Mark II detector[5] quite difficult. The difficulty is compounded at these low visible energies by large backgrounds from two-photon processes.

This search uses a new discriminant to extract the signal for heavy-lepton production from the two-photon backgrounds. The new requirement is the presence of an isolated, energetic photon as an indication of electromag-

 ©1990 The American Physical Society

netic radiation from the initial-state electron or positron (for very heavy leptons, final-state radiation is negligible). Demanding the isolated photon be produced at large angles with respect to the beam axis suppresses the two-photon background far more than it does the heavy lepton signal.

The large suppression can be understood from the following argument. Two-photon cross sections are large because the two virtual photons typically have an invariant mass squared very near zero, making them "quasi-real." The emission of an energetic photon from an incoming or outgoing electron, however, ensures that at least one virtual photon must have an invariant mass squared that is large and negative, suppressing the nominal two-photon cross section by many orders of magnitude. There remain backgrounds from two-photon processes with radiation emitted by charged particles created from the coalesced photons, but these backgrounds are quite small and relatively easy to remove through kinematic requirements. The "radiative tag," together with additional topological and kinematic requirements, provides sensitivity to near-degenerate lepton doublets without the necessity of electron or muon identification.

II. PROPERTIES OF NEAR-DEGENERATE LEPTON DOUBLETS

A. Decay modes

Reference 1 discussed in some detail the properties of sequential lepton doublets, with nonzero neutrino masses. The formulas given there for decay rates of the charged lepton into its neutral partner and conventional particles are used here. For the near-degenerate case, only four decay channels are important (charge-conjugate reactions are assumed throughout this paper):

$$L^- \to L^0 e^- \bar{\nu}_e \ , \tag{2}$$

$$L^- \to L^0 \mu^- \bar{\nu}_\mu \ , \tag{3}$$

$$L^- \to L^0 \pi^- \ , \tag{4}$$

$$L^- \to L^0 \rho^- (\to \pi^- \pi^0) \ . \tag{5}$$

In each of these cases, only a single charged particle is emitted from each charged heavy lepton. The branching ratios for these decay modes and others which are important at large δ are plotted versus δ in Fig. 1 for a charged-lepton mass of 10 GeV/c^2. The branching ratios are very sensitive to δ and relatively insensitive to m_-.

B. Production cross sections

For this search it is necessary to calculate the cross section

$$\sigma(e^+e^- \to L^+ L^- \gamma_{\rm tag}) \ ,$$

where $\gamma_{\rm tag}$ is a photon satisfying the radiative-tag requirements on direction and energy. Lowest-order exact formulas for this cross section can be found in Ref. 6. It is necessary, however, to include higher-order radiative corrections, to allow for emission of additional photons

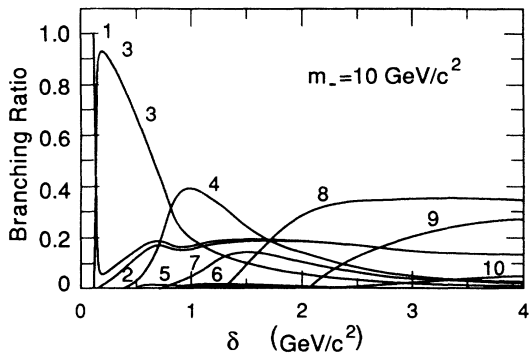

FIG. 1. Branching ratios for various heavy-charged-lepton decay modes plotted vs δ for a charged-lepton mass of 10 GeV/c^2: (1) $L^- \to \nu_L e^- \bar{\nu}_e$; (2) $L^- \to \nu_L \mu^- \bar{\nu}_\mu$; (3) $L^- \to \nu_L \pi^-$; (4) $L^- \to \nu_L \rho^-$; (5) $L^- \to \nu_L K^-$; (6) $L^- \to \nu_L K^{*-}$; (7) $L^- \to \nu_L a_1^-$; (8) $L^- \to \nu_L \bar{u}d$; (9) $L^- \to \nu_L \bar{c}s$; (10) $L^- \nu_L \tau^- \bar{\nu}_\tau$. Only the first four modes are important for $\delta < 1$ GeV/c^2. The quark-antiquark decays (8), followed by hadronization, do not include the exclusive hadronic decays simulated explicitly.

during the heavy-lepton pair production, photons that are undetected or mistaken for decay products of one of the charged leptons. We estimate the radiative corrections arising from initial-state radiation and from initial-state virtual corrections according to the prescription of Ref. 7, where we use the formulas of Ref. 6 in calculating the lowest-order cross sections. This approach is far from exact and somewhat sensitive to detector acceptance. From calculating the radiative correction for varying event selection cuts we estimate a systematic error on the total cross section, including radiative corrections that are no greater than 10%. For the requirements

$$|\cos\theta_{\rm tag}| < 0.70 \ , \tag{6}$$

$$E_{\rm tag} > 850 \text{ MeV} \ , \tag{7}$$

we find the lowest-order and radiatively corrected cross sections (initial-state radiation only) shown in Fig. 2. Final-state radiation is included after event generation

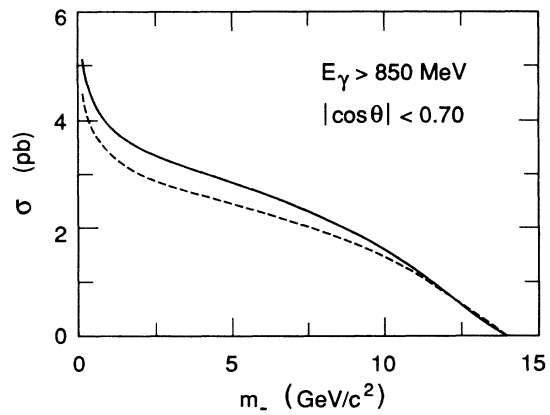

FIG. 2. Lowest order (dashed curve) and radiatively corrected (solid curve) cross sections for radiative charged-lepton pair production plotted vs charged-lepton mass, where the visible tagging photon must satisfy $|\cos\theta_{\rm tag}| \le 0.70$ and $E_{\rm tag} \ge 1$ GeV.

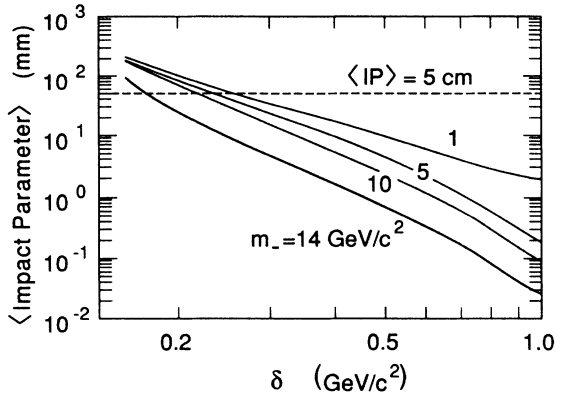

FIG. 3. Average impact parameter of pions from the decay $L^- \to L^0\pi^-$ plotted vs δ for various charged-lepton masses. Requiring detected charged tracks have an impact parameter less than 5 cm leads to poor detection efficiency for δ less than ≈ 250 MeV/c^2.

through an event-by-event weighting algorithm that depends on the kinematic configuration of the generated charged-lepton pair and photon, using the formulas of Ref. 6.

The event generator includes the correlations in momenta of decay products from the L^- and L^+, arising from weak effects in both production and decay.[8] Formulas may be found in Ref. 1.

C. Finite-lifetime effects

For very low mass differences, the total decay width of the heavy charged lepton becomes small enough that its finite lifetime leads to serious detection inefficiencies. Because the decay products can originate at a point displaced from the beam collision spot, their extrapolated trajectories are not in general consistent with having passed through that beam spot, a requirement of the Mark II charged-particle trigger.[9] Figure 3 shows the average distance of closest approach to the true beam spot of pions from the decay (4) plotted versus δ for various values of m_-. Since the Mark II trigger efficiency is poorly understood for tracks with impact parameters greater than 5 cm, this analysis uses only tracks with smaller impact parameters. From Fig. 3 one can see this implies poor sensitivity to lepton doublets with δ below ≈ 250 MeV/c^2.

D. Event signatures

Since in the nearly degenerate case, single-prong decays predominate, and since in each event two or more neutrinos or antineutrinos are undetected, the characteristic event signature of such heavy-lepton pair production is a pair of oppositely charged acollinear particles, sometimes accompanied by neutral pions. Because the heavy neutrinos carry away most of the available energy, these two tracks have low momenta. The additional requirement of an isolated, energetic photon leads to a distinct event signature with low backgrounds, as discussed in the next section.

III. EVENT SELECTION AND ANALYSIS

A. Data sample

We use e^+e^- annihilation data taken at $\sqrt{s} = 29$ GeV with the Mark II detector at the SLAC e^+e^- storage ring PEP in the detector's "preupgrade" configuration.[2] A detailed description can be found in Ref. 2. The following is a brief description of those elements important to this analysis.

Two cylindrical drift chambers concentric with the beam line provide charged-particles tracking in a 2.35-kG solenoidal magnetic field. The inner vertex chamber contains seven axial sense-wire layers; the outer chamber has ten stereo and six axial layers. Together they yield a momentum resolution $\delta p/p = [(0.025)^2 + (0.01p)^2]^{1/2}$ (p in GeV/c) in the plane transverse to the beam direction. Between the main drift chamber and the magnetic coil are 48 plastic scintillator counters that measure the time of flight (TOF) of charged particles originating from the collision point. These counters form part of the experiment's charged track trigger.

Immediately surrounding the magnetic coil are eight lead–liquid-argon calorimeter modules which cover 64% of the solid angle and have an energy resolution for photons of $\delta E/E \approx 0.14/\sqrt{E}$ (E in GeV). Unfortunately, gaps between the eight modules give rise to regions of poor resolution subtending 13% of the azimuth about the beam direction. Surrounding the calorimeter are four layers of steel and proportional tubes, providing reliable muon identification over 45% of the solid angle for high-momentum tracks. For this analysis, where charged-particle momenta are typically less than 2 GeV/c, the muon layers serve only as a tag for vetoing cosmic-ray backgrounds. At low forward angles reside the small-angle-tagger (SAT) detectors. Three sets of planar drift chambers allow tracking of low-angle charged particles. These chambers are followed by plastic scintillators and a calorimeter consisting of a sandwich of lead and plastic scintillator layers. Because of noise and low efficiency, the SAT drift chambers are not used in this analysis, but the scintillators and calorimeter provide a veto against certain two-photon backgrounds and events with very energetic, low-angle, initial-state radiation.

Although our earlier study[1] was based on a sample of 205.1 ± 3.0 pb^{-1}, much of the data was taken with reduced main-drift-chamber high voltage, leading to poorer triggering and track reconstruction efficiencies. Since the analysis presented here is quite sensitive to uncertainties in those efficiencies, we choose to use only a sample of data (104.0 ± 1.6 pb^{-1}) taken after the main drift chamber returned to full chamber voltage.

B. Expected backgrounds

A number of backgrounds were considered in this analysis from both annihilation and two-photon processes. Only four were found to be appreciable.

1. $e^+e^-\to\tau^+\tau^-\gamma$

The dominant background comes from $e^+e^-\to\tau^+\tau^-\gamma$. This background has been determined from Monte Carlo[1] simulation of τ pair production, including initial-state radiation. As in the heavy-lepton simulation, final-state radiation is included through an event-by-event weighting algorithm.

2. $e^+e^-\to e^+e^-\tau^+\tau^-$

In general, two-photon backgrounds are a major concern. Besides events with radiation from the electron or positron, which are largely suppressed by fiducial requirements on the tagging photon, there remain backgrounds due to final-state radiation emitted by particles formed by the coalesced photons. In addition, there are backgrounds from photons produced in the decay of neutral pions. Most of these backgrounds can be removed by requiring that the event's missing momentum transverse to the beam direction be relatively large, since two-photon events typically are characterized by small missing transverse momenta.

An exception, however, is the background from $e^+e^-\to e^+e^-\tau^+\tau^-$, which naturally has large missing momentum because of the undetected neutrinos produced. The tagging photon in this background arises mainly from the decay $\pi^0\to\gamma\gamma$, where one photon has too little energy to be detected, and where the π^0 is produced in the decay sequence:

$$\tau^-\to\nu_\tau\rho^-\to\nu_\tau\pi^-\pi^0 . \tag{8}$$

In annihilation production of tau pairs, the analogous background from τ decays to the ρ are negligible since the Lorentz boost of the high-energy τ's preclude the detected photons from satisfying isolation requirements. The background from $e^+e^-\to e^+e^-\tau^+\tau^-$ has been simulated with a Monte Carlo program,[10] using the double-equivalent-photon approximation.[11]

3. $e^+e^-\to e^+e^-\pi^+\pi^0\pi^0\pi^0$

A small background is expected from the process $e^+e^-\to e^+e^-\pi^+\pi^0\pi^-\pi^0$, where both π^0's decay into photon pairs, and where one photon satisfies the tagging requirements while at least one other photon escapes detection through a gap in the electromagnetic calorimeter acceptance, giving rise to large missing momentum. This process has been simulated with the same Monte Carlo program[10] used for the $e^+e^-\to e^+e^-\tau^+\tau^-$ background, where the cross section has been normalized according to measurements by the JADE and ARGUS experiments.[12,13]

4. $e^+e^-\to q\bar{q}\gamma$

Accurately predicting backgrounds from hadronic event production is quite difficult. One reason is that the LUND Monte Carlo program[14] used to simulate quark-antiquark production and subsequent "hadronization" has not been verified to the level of accuracy necessary in treating events with only two charged tracks. Another difficulty is that interactions of neutral hadrons in the Mark II electromagnetic detector are not simulated in this analysis. Although such simulations can be performed we cannot directly verify their accuracy from the data. For these reasons, the estimate presented below for hadronic backgrounds is not used in setting limits on new-heavy-lepton production. This is a conservative choice, since inclusion of additional background estimates would improve derived upper limits on production cross sections.

C. Selection of signature events

As described earlier, we search for events with two acollinear charged particles and at least one isolated, energetic photon. In order to ensure very high trigger efficiency, thereby reducing dependence upon Monte Carlo trigger simulation, each reconstructed charged track must satisfy stringent requirements.

(1) The track momentum must make an angle greater than 45° with respect to either beam direction.

(2) The momentum transverse to the beam ($p_\perp$) must be greater than 150 MeV.

(3) There must be a signal from both photomultiplier tubes of the TOF counter in the track's projected path. In addition, the measured flight time must be in the range 0–12 ns.

(4) The track must have at least 10 associated drift-chamber signals (out of a possible 23), and at least one of those signals must come from one of the four inner layers of the vertex chambers.

(5) The χ^2 per degree of freedom calculated from the helical track fit to the drift-chamber signals must be less than 5.

(6) The impact parameter of the track with respect to the beam collision point in the plane transverse to the beam direction must be less than 5 cm. From measurement of K_S^0 decays in two-photon events from the data we also find a trigger inefficiency that depends upon the angle between a particle's initial direction of motion at production and the direction of that production point with respect to the beam collision point. To reduce sensitivity to this inefficiency, we place a requirement on a variable that depends on the particle's transverse momentum, its charge, and the location of its point of closest approach to the beam axis. More detail can be found in Ref. 15.

In addition to these fiducial and track quality requirements, the tracks must have a total measured momentum less than 4 GeV/c, and any energy in the electromagnetic calorimeter associated with the track must be less than 4 GeV. These requirements select events with low visible energy, filtering out backgrounds from radiative τ pair production and from mismeasured radiative Bhabha and μ pair production.

In order to reduce backgrounds from π^0 decays, we require the tagging photon to be isolated both from charged tracks and from other detected photons. To ensure reliable Monte Carlo simulation of calorimeter response, we also require that the photon satisfy tight fiducial requirements.

(1) The measured energy must be at least 1 GeV.

(2) The photon polar angle θ_γ with respect to the beam must satisfy $|\cos\theta_\gamma| \leq 0.66$.

(3) The photon's azimuth direction must be at least 3° away from the center of the nearest crack between calorimeter modules.

(4) The total reconstructed energy deposition in the calorimeter within 30° of the photon must be less than 150 MeV.

(5) No reconstructed neutral in the calorimeter within 90° of the photon can combine with it to give an invariant mass consistent with a π^0 or η, where consistent means

$$|M_{\gamma_1\gamma_2} - M_{\pi^0,\eta}| \leq \delta M_{\gamma\gamma} ,$$

where $\delta M_{\gamma\gamma}$ is the invariant-mass resolution for the two photons, and where for the η condition, the other photon must have an energy of at least 150 MeV.

(6) The angle between the photon and nearest charged track momentum must be at least 45°.

If more than one photon in an event satisfies the tagging requirements, the photon with the least total nearby (within 30°) neutral calorimetry energy is taken as the tag. If more than one eligible photon has no nearby neutral energy, the most energetic is taken as the tag.

Additional requirements are imposed on the topology of each candidate event, designed both to suppress various backgrounds and to ensure reliable measurement. Because charged tracks passing near one another may induce a signal on the same drift-chamber wire or on neighboring wires, creating confusion during track reconstruction, we impose cuts on the minimum opening angle between the two allowed charged tracks. In the plane transverse to the beam, the opening angle must be at least 5.7°, and in three dimensions must be at least 20°.

We also impose cuts on the maximum opening angle between the two tracks. In order to suppress backgrounds from two-photon processes where the tagged photon candidate production is unrelated to the charged-particle productions (e.g., cosmic-ray coincidences, to be discussed later), we require the acoplanarity (180° minus the opening angle in the transverse plane) be greater than 1.1°. In order to suppress further the backgrounds from radiative τ pair and radiative Bhabha production we require the opening angle between the tracks in three dimensions be less than 160°.

In order to suppress radiative τ pair production accompanied by decays involving one or more π^0's, the total neutral energy of the event, excluding the contribution from the tagging photon, must be less than 2 GeV. As discussed earlier, two-photon backgrounds typically have low missing transverse momentum. Hence, we require the missing transverse momentum of the event be greater than 1 GeV/c. Similarly, the direction of the total detected momentum must make an angle greater than 45° with respect to the beam axis. These last two requirements also suppress events with very hard initial-state radiation along one of the beam directions.

Because energetic photons can escape detection through gaps in azimuth between calorimeter modules, leading to apparent missing transverse momentum, we also require that the missing transverse momentum point

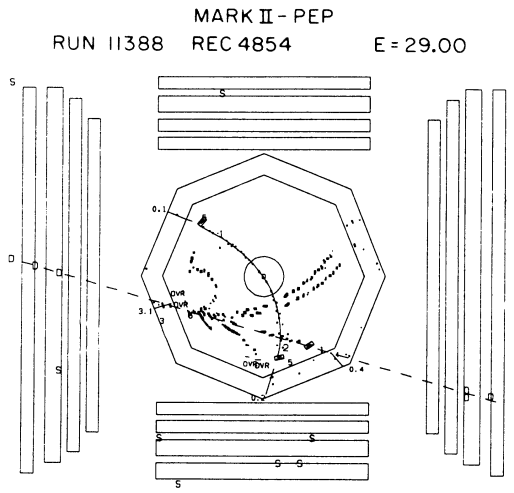

FIG. 4. Example of unusual background event, where a cosmic-ray muon enters the detector from the left and induces an electromagnetic shower in the calorimeter, which in this case, leaks into the central drift chamber. At the same time, an electron-positron collision in the center produces a coplanar charged track pair through a two-photon process. The dashed line shows a fit to the three muon chamber signals at the left (indicated by D). The line passes through the "tagged photon" candidate which is reconstructed to have an energy of 3.1 GeV. This event is the only event to be flagged by all three of the cosmic veto algorithms described in the text.

at least 3° away from the center of the nearest gap. Two-photon processes sometimes produce at low angles an electron or positron that can be detected by the SAT system. Such events are enhanced relative to untagged events by the above requirements of missing transverse momentum in the central detector. Similarly, hard initial-state radiation can produce a photon detectable with the SAT calorimeter. In order to suppress such backgrounds we require the total SAT detected energy be less than 8 GeV. In addition, if one of the plastic scintillators placed in front of the SAT calorimeters detects a charged particle in coincidence with a measured calorimeter energy greater than 200 MeV, the event is discarded.

Another background, peculiar to this analysis, comes from a cosmic-ray muon inducing an electromagnetic shower in the calorimeter, in coincidence with an electron-positron interaction that produces two charged particles in the central detector. The cosmic-ray shower (due to a "knock-on" electron) is reconstructed and misinterpreted as a photon, since typically there is no charged track leading from the beam collision point to the shower region. An example of such an event is shown in Fig. 4, where the dashed line indicates the deduced trajectory of the muon that caused the false photon shower.

In order to remove these events we veto any event that is flagged by one or more of three algorithms. These three algorithms are based on excess energy deposition near the tagged photon candidate, inconsistent with a photon originating from the beam collision, on alignment of unassociated drift-chamber signals with the tagging photon, and on alignment of unassociated muon chamber signals with the tagging photon.

TABLE I. Expected backgrounds to candidate events in 104 pb^{-1}. Note that the last background (radiative quark-antiquark production) is not included in the total and is not used in setting limits on new-heavy-lepton production.

$e^+e^- \to \tau^+\tau^-\gamma$	9.7±1.4
$e^+e^- \to e^+e^-\tau^+\tau^-$	2.3±1.0
$e^+e^- \to e^+e^-\pi^+\pi^0\pi^-\pi^0$	0.3±0.2
$e^+e^- \to q\bar{q}\gamma$	1.7
Total	12.3±1.7

IV. RESULTS AND CONCLUSIONS

A. Numerical results

After all selection cuts, 14 events remain from 104-pb^{-1} of data. Table I shows the estimated backgrounds from the four processes discussed earlier. Ignoring the estimate for hadronic backgrounds for reasons discussed above we expect a total of 12.3±1.7 events from conventional processes, consistent with what we observe in the data. Figure 5 shows the distribution in tagging photon energy for the data (plotted points) and for the sum of the first three backgrounds (histogram). Figure 6 shows the distribution in invariant mass of the two charged particles for both data and background. Figure 7 shows the distribution in reconstructed charged track momentum (two entries/event) for both data and estimated background. We see no significant deviations between the data and estimated background for these or any other distributions we have examined.

As a further check we have applied an algorithm[16] that identifies electrons and pions with 60–90% efficiency and misidentification probabilities less than 15% for tracks with low momenta. Based upon energy deposition and shower shape in the calorimeter and upon measured charged-particle flight times, the algorithm was developed and checked with data taken with the Mark II detector at the SLAC storage ring SPEAR at $\sqrt{s} = 3.1$ GeV. Table II shows that there is good agreement between the data and estimated backgrounds (shown in parentheses) in the pattern of identified particle combinations.

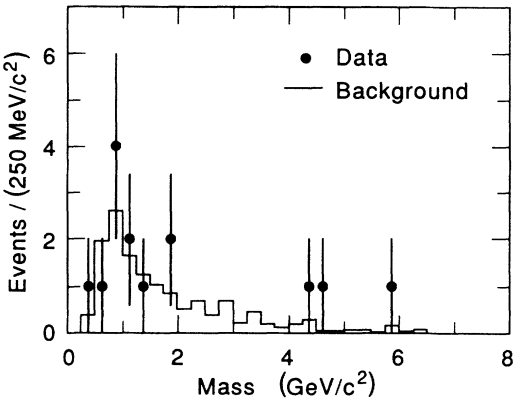

FIG. 6. Distribution in invariant mass of two charged tracks for final candidate events in the data (points) and the expected background (histogram).

B. Limits on new-lepton pairs

Having found no significant evidence for a new heavy lepton doublet we next determine the (m_-, δ) region we can exclude with this analysis. Monte Carlo simulations of $e^+e^- \to L^+L^-\gamma$ were made at the 86 points in the (m_-, δ) plane shown in Tables III–VI. The simulated L^+L^- production included initial-state and final-state radiation, and the decays were performed according to the formulas given in Ref. 1. All Monte Carlo events were subjected to the same analysis requirements imposed on the data.

There are in general many approaches to setting limits on new-heavy-lepton production. For example, one can compare shapes or total numbers of events between data and the sum of expected backgrounds and a hypothetical heavy-lepton signal for one or more distributions such as

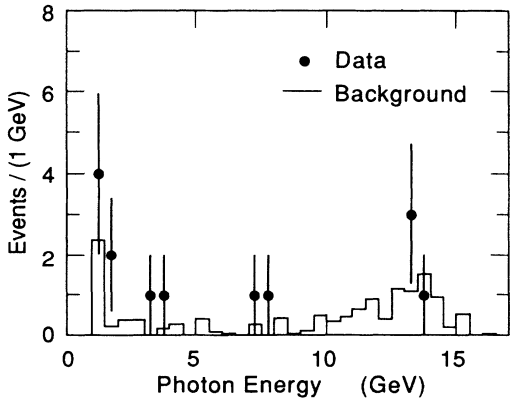

FIG. 5. Distribution in tagged-photon energy for final candidate events in the data (points) and the expected background (histogram).

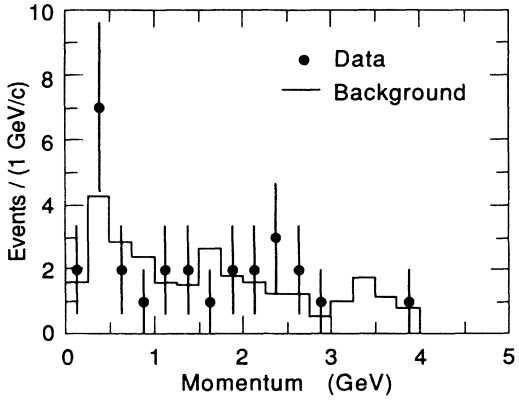

FIG. 7. Distribution in charged-track momentum (two entries/event) for final candidate events in the data (points) and the expected background (histogram).

TABLE II. Distribution in identified electrons, pions, and ambiguous particles for the final candidate sample from the data and from the backgrounds (shown in parentheses).

	Particle identity		
	Electron	Pion	Ambiguous
Electron	1(0.7)	1(2.6)	2(1.0)
Pion	—	4(3.3)	4(3.1)
Ambiguous	—	—	2(1.5)

those in Figs. 5–7. We take the simplest and somewhat conservative approach of comparing only total numbers of events.

Since the number of surviving events in this analysis is quite low, it is necessary to apply techniques based on Poisson statistics. We define the integrated joint probability $P(\lambda, N_D)$ for observing N_D or fewer events, given a Monte Carlo estimate λ with error σ_λ, according to the formula

$$P(\lambda, N_D) = \frac{1}{\sqrt{2\pi}\,\sigma_\lambda} \int_0^\infty d\lambda' \exp\left[-\frac{(\lambda'-\lambda)^2}{2\sigma_\lambda^2} - \lambda' \right] \sum_{i=0}^{N_D} \frac{(\lambda')^i}{i!}, \tag{9}$$

where we integrate over all possible values of the true expectation value λ', weighting according to the likelihood

TABLE III. Expected number of signal events with errors and confidence levels of exclusion for the generated Monte Carlo samples with mass differences of 0.2 and 0.3 GeV/c^2. Estimated errors on average expected numbers of events are systematic only; they do not include statistical fluctuations in observed numbers of events.

δM (GeV)	M_L (GeV)	Number of events	C.L. (%)
0.2	1.0	6.5±1.1	74.3
0.2	2.0	11.8±1.9	95.6
0.2	3.0	11.2±1.8	94.5
0.2	4.0	10.0±1.6	91.6
0.2	5.0	8.5±1.3	86.4
0.2	6.0	7.8±1.2	82.9
0.2	8.0	4.4±0.7	55.1
0.2	10.0	2.2±0.4	27.9
0.2	11.0	1.1±0.2	14.2
0.2	12.0	0.6±0.1	7.3
0.3	0.3	0.5±0.2	5.8
0.3	1.0	24.2±3.5	>99.9
0.3	2.0	42.8±6.2	>99.9
0.3	3.0	36.0±5.2	>99.9
0.3	4.0	33.5±4.9	>99.9
0.3	5.0	29.0±4.2	>99.9
0.3	6.0	25.2±3.7	>99.9
0.3	8.0	16.3±2.4	99.3
0.3	10.0	8.6±1.3	86.9
0.3	11.0	6.0±0.9	70.8
0.3	12.0	3.6±0.5	46.2

TABLE IV. Expected number of signal events with errors and confidence levels of exclusion for the generated Monte Carlo samples with mass differences of 0.8 and 0.6 GeV/c^2.

δM (GeV)	M_L (GeV)	Number of events	C.L. (%)
0.4	0.4	1.9±0.4	24.9
0.4	1.0	32.8±4.5	>99.9
0.4	2.0	52.2±7.2	>99.9
0.4	3.0	50.3±6.9	>99.9
0.4	4.0	44.9±6.2	>99.9
0.4	5.0	36.3±5.0	>99.9
0.4	6.0	30.7±4.3	>99.9
0.4	8.0	19.6±2.8	99.8
0.4	10.0	11.6±1.6	95.5
0.4	11.0	7.2±1.0	79.4
0.4	12.0	4.1±0.6	51.9
0.6	0.6	13.2±1.9	97.5
0.6	1.0	26.4±3.4	>99.9
0.6	2.0	45.6±5.8	>99.9
0.6	3.0	49.5±6.3	>99.9
0.6	4.0	49.0±6.3	>99.9
0.6	5.0	38.2±4.9	>99.9
0.6	6.0	33.7±4.3	>99.9
0.6	8.0	20.8±2.7	>99.9
0.6	10.0	11.9±1.5	96.1
0.6	11.0	7.5±1.0	81.7
0.6	12.0	3.8±0.5	49.0

TABLE V. Expected number of signal events with errors and confidence levels of exclusion for the generated Monte Carlo samples with mass differences of 0.8, 1.0, and 1.2 GeV/c^2.

δM (GeV)	M_L (GeV)	Number of events	C.L. (%)
0.8	0.8	16.5±2.2	99.4
0.8	1.0	17.9±2.3	99.7
0.8	2.0	30.7±4.0	>99.9
0.8	3.0	37.2±4.9	>99.9
0.8	4.0	40.5±5.4	>99.9
0.8	5.0	34.0±4.6	>99.9
0.8	6.0	28.6±3.9	>99.9
0.8	8.0	19.7±2.7	99.8
0.8	10.0	10.6±1.4	93.6
0.8	11.0	6.6±0.9	75.8
0.8	12.0	3.6±0.5	46.5
1.0	1.0	13.8±1.2	98.4
1.0	2.0	20.9±2.0	>99.9
1.0	3.0	28.1±2.7	>99.9
1.2	1.2	12.8±1.7	97.1
1.2	2.0	17.9±2.5	99.6
1.2	3.0	25.8±3.5	>99.9
1.2	4.0	27.8±3.7	>99.9
1.2	5.0	25.3±3.5	>99.9
1.2	6.0	24.1±3.3	>99.9
1.2	8.0	17.1±2.4	99.5
1.2	10.0	9.2±1.3	89.2
1.2	11.0	6.0±0.8	70.4
1.2	12.0	3.1±0.4	40.3

TABLE VI. Expected number of signal events with errors and confidence levels of exclusion for the generated Monte Carlo samples with mass differences of 1.4, 1.6, 1.8, and 2.0 GeV/c^2.

δM (GeV)	M_L (GeV)	Number of events	C.L. (%)
1.4	3.0	17.8±1.6	99.8
1.4	4.0	20.9±1.9	>99.9
1.4	5.0	21.1±1.9	>99.9
1.4	6.0	18.8±2.5	99.8
1.6	2.0	12.4±1.7	96.7
1.6	3.0	13.9±1.8	98.2
1.6	4.0	15.8±2.1	99.2
1.6	5.0	15.5±2.1	99.0
1.6	6.0	15.7±2.0	99.1
1.6	8.0	12.1±1.6	96.4
1.6	10.0	7.3±1.0	80.2
1.6	11.0	4.7±0.6	58.2
1.6	12.0	2.5±0.3	32.4
1.8	4.0	12.5±1.1	97.2
1.8	5.0	14.0±1.8	98.2
1.8	6.0	14.0±1.8	98.3
1.8	8.0	10.3±1.4	92.8
2.0	5.0	11.1±1.0	95.0
2.0	6.0	10.1±0.9	92.8

that the true λ' would lead to our Monte Carlo estimate λ. The summation in the integrand arises from the Poisson probability of observing N_D or fewer events, given an expectation of λ'. (When σ_λ is a significant fraction of λ, the normalization constant in front of the integral must be adjusted.) For illustration, the joint probability that we would observe 14 events or fewer is calculated to be 73%, given our background estimate of 12.3±1.7. If there is no signal, and expected backgrounds have been calculated correctly, one expects an average probability near 50%.

We take as our confidence level for excluding a hypothetical heavy-lepton signal the expression

$$1-\frac{P(\lambda_T,\sigma_T,N_D)}{P(\lambda_B,\sigma_B,N_D)}, \tag{10}$$

where $\lambda_B\pm\sigma_B$ is the expectation value of the background alone and $\lambda_T\pm\sigma_T$ is the expectation value of the background plus the signal. This expression gives a lower, more conservative confidence level than $1-P(\lambda_T,\sigma_T,N_D)$.

Tables III–VI show the expectation values and errors of the 86 Monte Carlo heavy-lepton samples generated for this analysis, along with the confidence levels for exclusion derived from formulas (9) and (10). Most of the lepton doublets for which Monte Carlo samples were generated can be excluded with greater than 99% confidence, although none with $\delta=200$ MeV/c^2 can be excluded with that confidence. Interpolation between these points in the (m_-,δ) plane yields contours of exclusion at fixed confidence levels. Within the two contours shown in Fig. 8 we exclude heavy lepton doublets with greater than 95% and 99% confidence. We are limited in sensitivity at high charged-lepton masses because production rates for charged fermion-antifermion pairs fall rapidly as the fermion mass-energy approaches the beam energy. As discussed earlier, we are limited at low δ by effects due to the finite lifetime of the heavy charged lepton. At mass differences much above 1 GeV/c^2, heavy lepton events have larger visible energies than permitted in this analysis.

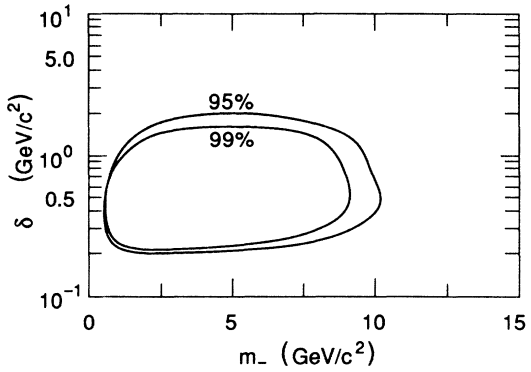

FIG. 8. Within the contours we exclude a new heavy lepton doublet with greater than 95% and 99% confidence level.

This analysis extends our limits on heavy-lepton-doublet production to a region of smaller δ than attained in our previous analysis[1] because the radiative tag precludes the necessity for electron or muon identification and for associated high visible energies. On the other hand, the new requirement of an isolated, energetic photon aggravates mass suppression effects, giving much-reduced sensitivity at very heavy lepton masses.

C. Conclusions

In conclusion, we have found no evidence for a nearly degenerate heavy-lepton doublet (L^-,L^0) in our 29-GeV annihilation data and have excluded this possibility for mass splittings (δ) as low as 250–400 MeV/c^2 for charged-lepton masses between 500 MeV/c^2 and 10 GeV/c^2.

In addition, we have investigated the value of radiative tagging in extracting low-visible-energy events from large two-photon backgrounds. We find the technique quite useful, but in our case, limited by reliance upon a charged track trigger, a serious drawback in searching for long-lived particles with decay points appreciably displaced from the beam collision spot. This technique could be better exploited by experiments possessing a trigger directly sensitive to the low-energy tagging photons.

ACKNOWLEDGMENTS

This work was supported in part by Department of Energy Contracts Nos. DE-AC03-76SF00515(SLAC) and DE-AC03-76SF00098(LBL).

[a]Present address: University of California, Riverside, CA 92521.
[b]Present address: University of California, Santa Cruz, CA 95064.
[c]Present address: University of Pennsylvania, Philadelphia, PA 19104.
[d]Present address: Indiana University, Bloomington, IN 47405.
[e]Present address: Carleton University, Ottawa, Ontario, Canada K1S 5B6.
[f]Present address: Boston University, Boston, MA 02215.
[g]Present address: University of Wisconsin, Madison, WI 53706.
[h]Present address: University of Chicago, Chicago, IL 60637.
[i]Present address: University of Florida, Gainesville, FL 32611.
[j]Present address: Fermilab, Batavia, IL 60510.
[k]Present address: University of Oklahoma, Norman, OK 73019.
[l]Present address: Therma-Wave Corporation, Fremont, CA 94539.
[m]Present address: Brookhaven National Laboratory, Upton, NY 11973.
[n]Present address: Columbia University, New York, NY 10027.
[o]Present address: California Institute of Technology, Pasadena, CA 91125.
[p]Present address: University of Illinois, Urbana, IL 61801.
[q]Present address: CERN, CH-1211, Genève 23, Switzerland.
[r]Present address: Université de Genève, CH-1211, Genève 4, Switzerland.

[1]D. Stoker *et al.*, Phys. Rev. D **39**, 1811 (1989).
[2]R. H. Schindler *et al.*, Phys. Rev. D **24**, 78 (1981).
[3]M. L. Perl, in *Proceedings of the XXIII International Conference on High Energy Physics,* Berkeley, California, 1986, edited by S. C. Loken (World Scientific, Singapore, 1987), p. 596.
[4]S. Raby and G. B. West, Nucl. Phys. **B292**, 793 (1987).
[5]M. Nelson, Ph.D. thesis, University of California, Berkeley, Report No. LBL-16724, 1983.
[6]F. A. Berends *et al.*, Acta Phys. Pol. **B14**, 413 (1983).
[7]G. Bonneau and F. Martin, Nucl. Phys. **B27**, 381 (1971).
[8]B. F. L. Ward, Phys. Rev. D **35**, 2092 (1987).
[9]H. Brafman *et al.* Report No. SLAC-PUB-2033, 1977 (unpublished).
[10]J. R. Smith, Ph.D. thesis, University of California, Davis, Report No. RX-1171, 1982.
[11]R. H. Dalitz and D. R. Yennie, Phys. Rev. **105**, 1598 (1957).
[12]H. Kolanoski, in *Photon Photon Collisions,* proceedings of the V International Workshop, Aachen, Germany, 1983, edited by C. Berger (Lecture Notes In Physics, Vol. 191) (Springer, Berlin, 1983).
[13]H. Albrecht *et al.*, Phys. Lett. B **217**, 205 (1989).
[14]T. Sjöstrand, Comput. Phys. Commun. **39**, 347 (1986); A. Bäcker, Z. Phys. C **12**, 161 (1982).
[15]K. Riles, Ph.D. thesis, Stanford University, SLAC Report No. 342, 1989.
[16]J. Dorfan, internal Mark II memo, 1979 (unpublished).